J Mater Sci (2011) 46:4812–4819
DOI 10.1007/s10853-011-5391-1

Alumina microtubes prepared via template-directed pulsed chemical vapor deposition (pulsed CVD)

Amit K. Roy · Stefan Knohl · Werner A. Goedel

Received: 30 November 2010 / Accepted: 11 February 2011 / Published online: 4 March 2011

Abstract Bundles of alumina microtubes were prepared by depositing alumina onto bundles of "endless" carbon fibers via pulsed chemical vapor deposition and subsequent removal of the fibers. Thin alumina films were deposited onto "endless" carbon fibers at 77 °C by gas phase exposures to sequential pulses of trimethylaluminum and water vapor, respectively. The carbon fibers were selectively removed using thermal oxidation in air at temperatures exceeding 550 °C. The length of the tubes was primarily limited by the dimension of the used furnace. The longest tubes thus had a length of 30 cm. Scanning electron microscopic (SEM) images of the microtubes revealed that each individual tube was separated from its neighbors and that the tubes had an almost uniform wall thickness. SEM and transmission electron microscopic (TEM) images indicate that the inner side of the wall has the same morphology as the fiber template. As deposited, the alumina films have a predominantly amorphous structure; this is transformed into a polycrystalline structure during thermal oxidation. At low thermal oxidation temperatures, such as 550 °C, the alumina microtubes still comprise a substantial fraction of amorphous structure, at higher oxidation temperatures, 900 °C or above, a dominating polycrystalline structure (with bigger grains) is formed. This transformation gives rise to grain boundaries. These grain boundaries might facilitate oxygen diffusion and thus oxidative removal of the fiber templates.

A. K. Roy · S. Knohl · W. A. Goedel (✉)
Physical Chemistry, Institute of Chemistry, Chemnitz University of Technology, Strasse der Nationen 62,
09111 Chemnitz, Germany
e-mail: werner.goedel@chemie.tu-chemnitz.de

Introduction

Pulsed chemical vapor deposition (pulsed CVD) is a sequential chemical vapor deposition (CVD): at least two precursors are delivered to a surface in separate pulses [1], each pulse separated from the subsequent one by an evacuation period. Often in this evacuation period, the reaction chamber is purged by an inert gas to remove excess precursor from the reaction chamber. Due to this evacuation period, one can control the degree of mixing of the precursors in the gas phase, and thus the amount deposited per cycle. In its extreme, called atomic layer deposition (ALD), (i) no mixing of the precursors occurs in the gas phase and thus mutual chemical reactions in the gas phase are prevented and (ii) each of the precursors reacts with the surface to form a layer of limited growth (ideally a monolayer) and activates the surface for reaction with the subsequent precursor pulse. Since the growth per pulse is limited, one obtains uniform film thickness all over the samples, regardless of the path that the precursors have to diffuse through to reach the surface. On the other hand, there are quite interesting deviations from this strict scheme. For example, one of the precursors might only deposit a catalyst to the surface while the other one gives rise to limited growth of more than a monolayer [2], or one can obtain limited growth (usually more than a monolayer) if the purging is chosen too short to prevent mixing in the gas phase completely.

Oxide microtubes and nanotubes are of interest because of their potential applications in solar energy conversion devices [3, 4], gas sensors [5, 6], single-DNA sensing [7], molecular separation [8], and drug delivery systems [9]. Microtubes and nanotubes can be synthesized by (i) self-organization [10, 11], (ii) deposition from spherical catalysts [12, 13], (iii) by rolling up thin solid films [14], (iv)

covering the walls of cylindrical pores, or (v) covering cylindrical fibers [15]. The last two methods are known as "template-directed" synthesis. Templates should have such a property that they can withstand the deposition conditions and can easily be removed after deposition without affecting the tubes. Various materials already have been used as templates such as nanorods, carbon nanotubes, electrospun fiber, porous media, etc. [15]. Compared to other methods, the template-directed route is of advantage because one can control the size and shape of the tubes easily. Several methods already have been applied to a template-directed synthesis of metal oxide microtubes, such as: sol–gel deposition [16], atmospheric chemical vapor deposition (atmospheric CVD) [17], and ALD [18]. Sol–gel deposition and atmospheric CVD often generate inhomogeneous films and the thickness of the walls varied from one tube to another. Microtubes are often bridged in these two methods. On the other hand, ALD and pulsed CVD have the advantage that one can produce microtubes of uniform wall thickness with smooth and homogeneous surfaces. However, the film deposition rate of ALD is quite slow, e.g., the average deposition rate of alumina onto electrospun poly(vinyl alcohol) fibers using trimethylaluminum and water is 0.08 nm/cycle [18], and 0.03 nm/cycle onto graphitic carbon fibers using aluminum chloride and water [19].

We are aware of one very carefully done publication on the preparation of microtubes via ALD deposition of alumina onto polymeric fibers [18]. In this study, it was shown that one can obtain tubes with controlled wall thickness. On the other hand, the template used was a felt of fibers, thus the tubes were limited in length, non-aligned, and not accessible as individuals. We recently showed that pulsed CVD can be used to coat "endless" fibers [19, 20]. Thus, the goal of our current contributions is to show, that one can produce "endless" microtubes, that are well aligned in bundles and in principle might be handled as individuals of several centimeters in length.

Experimental section

Tenax HTA 5331 6 K, PAN-based carbon fibers (bundle of approximately 6000 fibers, each fiber had a diameter of approximately 7 μm) were purchased from TOHO TENAX. As obtained, the fiber bundles bear a polymeric sizing. This sizing was removed by thermal treatment at 700 °C in N_2 atmosphere. Besides this thermal desizing no other treatment was performed before film deposition. The reaction chamber and sample holder are identical to the one described elsewhere [19]. Briefly, the reactor is a 1 m long steel tube connected at one end to the precursors via computer-controlled valves and to the purge gas via mass flow controllers and at the other end to a rotary vane pump (PFEIFFER VACUUM, Duo 5, Mod. Nr.: PK D61 705 AA) via another computer-controlled valve. 3.6 m long segments of this fiber were spooled onto a 30 cm long fiber holder in such a way that they were bent by 180° with a bending radius of 5 mm at both ends of the holder while being straight and parallel to each other between these two ends. The fiber holder was mounted into the reactor in such a way that the fibers were aligned parallel to the tube axis, one of the ends of the holder facing the precursor flow the other end facing the pump. Fibers are coated with alumina at a temperature of 77 °C using pulses of trimethylaluminum (98% from ABCR GmbH & co. KG, Karlsruhe) and of deionized water. The supply vessel of trimethylaluminum was heated to 60 °C. The temperature of the water supply was maintained at 50 °C. Two streams of nitrogen were used as carrier for trimethylaluminum and water, respectively, as well as purge gas; their flow was controlled by two mass flow controllers each set to 20 standard cubic centimeters per minute (sccm). In the first half cycle, the fiber bundle was exposed to trimethylaluminum for 20 s followed by purging the reactor with nitrogen for 30 s. In the second half cycle, it was exposed to water vapor for 20 s followed by purging the reactor with nitrogen for 30 s. From the vapor pressure of TMA (89.8 hPa [25]), respectively, water (123 hPa [26]) in the reservoirs and flow of carrier gas one can calculate a total exposure per cycle of 13.5×10^8 Langmuir of TMA and 18.5×10^8 Langmuir of water. In both exposures the valve in front of the pump was closed, it was opened fully during the purge time.

Carbon fibers were removed selectively after film deposition via thermal oxidation at temperatures exceeding 550 °C in air using a tube furnace.

To characterize films onto the fibers directly after deposition, SEM and EDXS were recorded using a Nano-NovaSEM (PHILIPS), specimens were taken from the bundles. To characterize tubes after thermal oxidation, TEM was recorded using a PHILIPS CM 20 FEG taking directly the microtubes. TEM images were recorded in transmission perpendicular to the natural surface of the coating.

Elemental flash analysis was performed via flash pyrolysis/oxidation of the sample, coupled to a chromatographic separation and detection of the gaseous oxidation products using a FLASHAE 1112 (Thermo SCIENTIFIC).

Result and discussions

Bundles of alumina microtubes were prepared by depositing alumina onto bundles of "endless" carbon fibers via pulsed CVD and subsequent removal of the fibers.

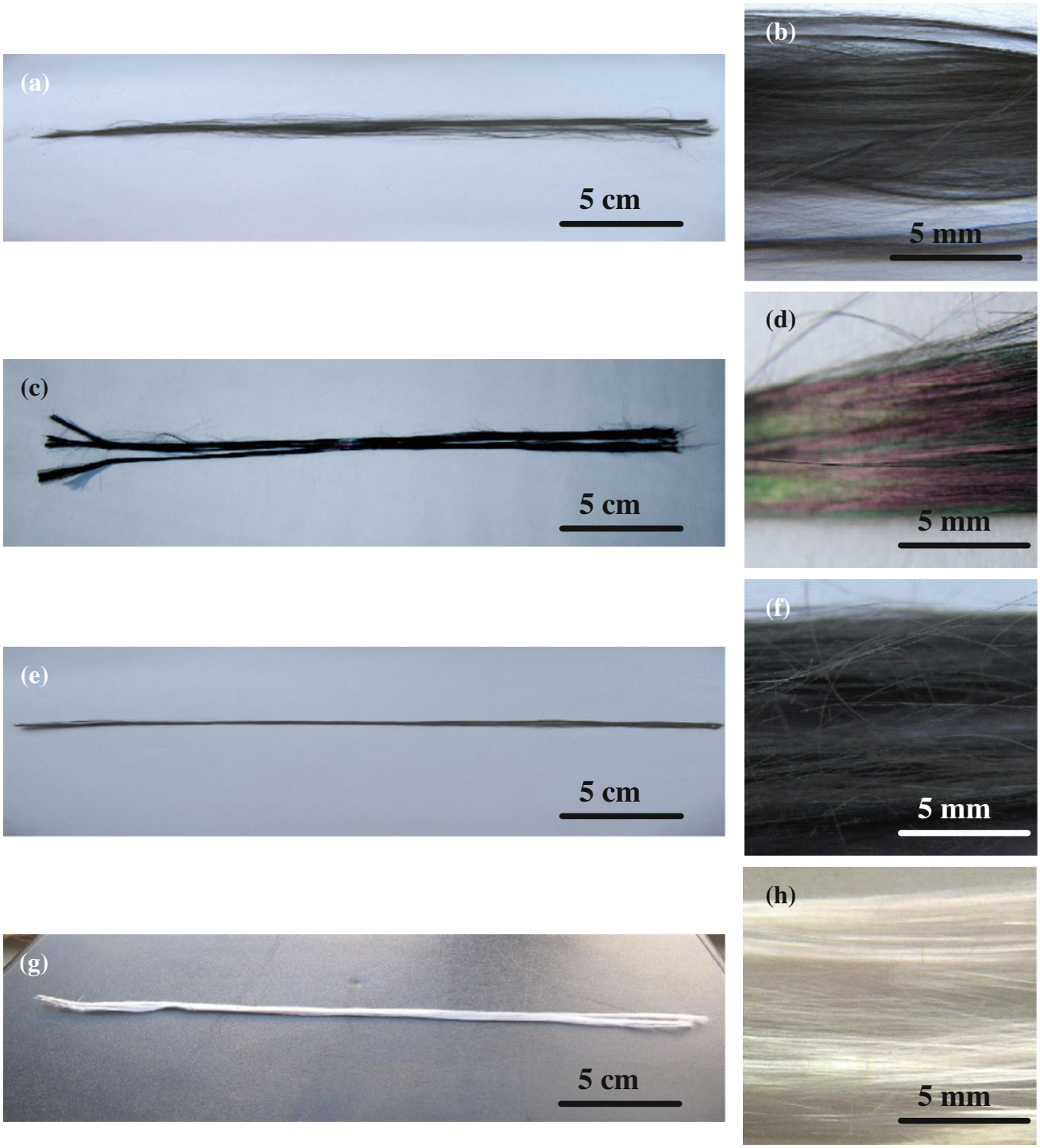

Fig. 1 Photographic images of (**a**), (**b**) carbon fibers before film deposition, (**c**), (**d**), carbon fibers after film deposition, (**e**), (**f**), at an intermediate stage of oxidation, (**g**), (**h**), microtubes

Fibers before film deposition

Before film deposition, the fibers have a black appearance and are aligned parallel to each other in bundles (see in Fig. 1a, b). Scanning electron microscopy (SEM) images of a part of a fiber bundle and a single fiber are shown in Fig. 2a, b, respectively. Individual fibers have a corrugated surface bearing grooves parallel to the fiber axis and irregular protuberances; this morphology varies from fiber to fiber. According to the literature, the fibers are composed

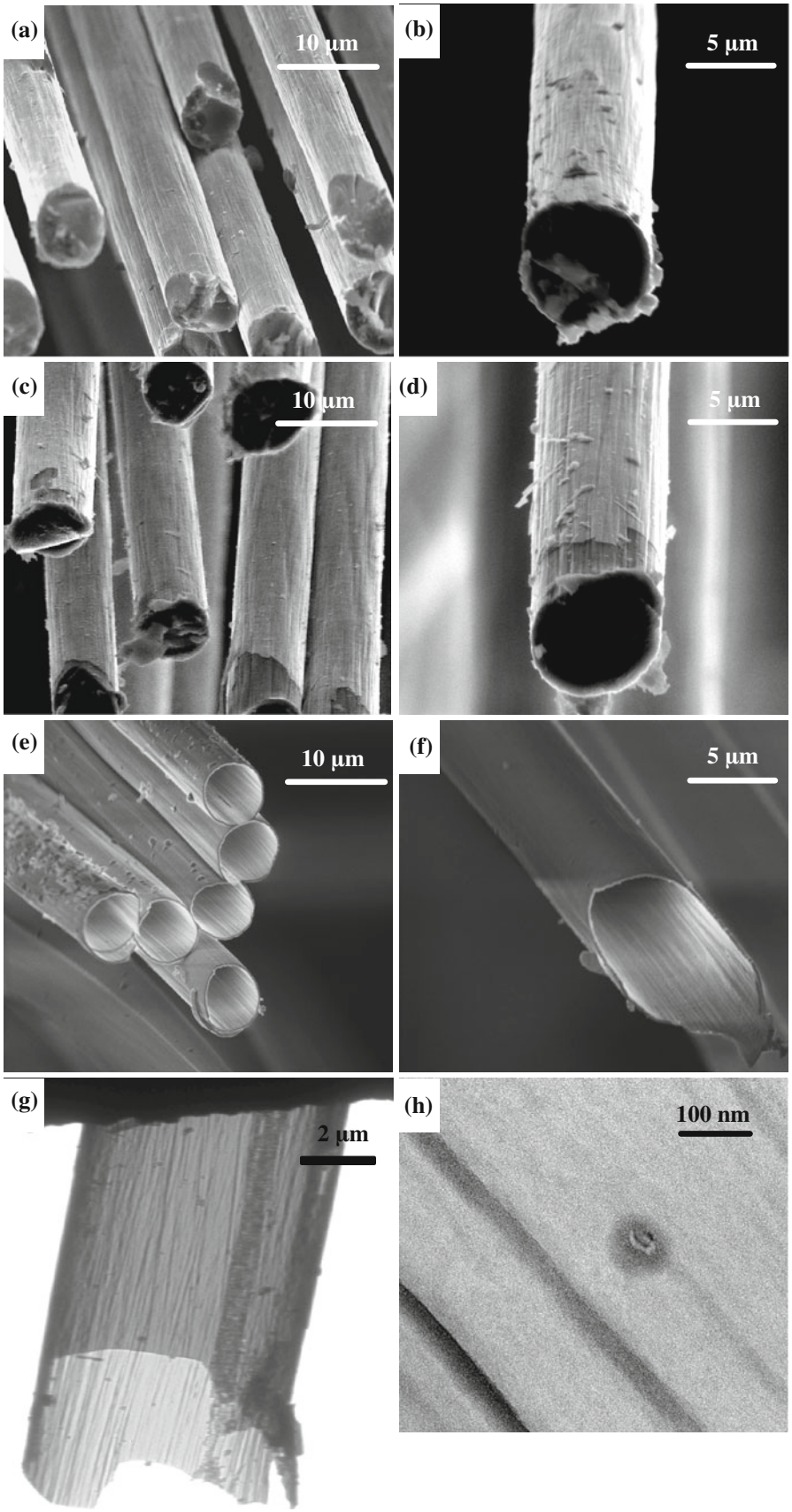

Fig. 2 Scanning electron microscopic (SEM) images of (**a**), (**b**) carbon fibers before thin film deposition, (**c**), (**d**) carbon fibers after thin film deposition, (**e**), (**f**) microtubes, and (**g**), (**h**) transmission electron microscopic (TEM) image of one microtube, (**g**) single microtube (**h**) a part of a microtube

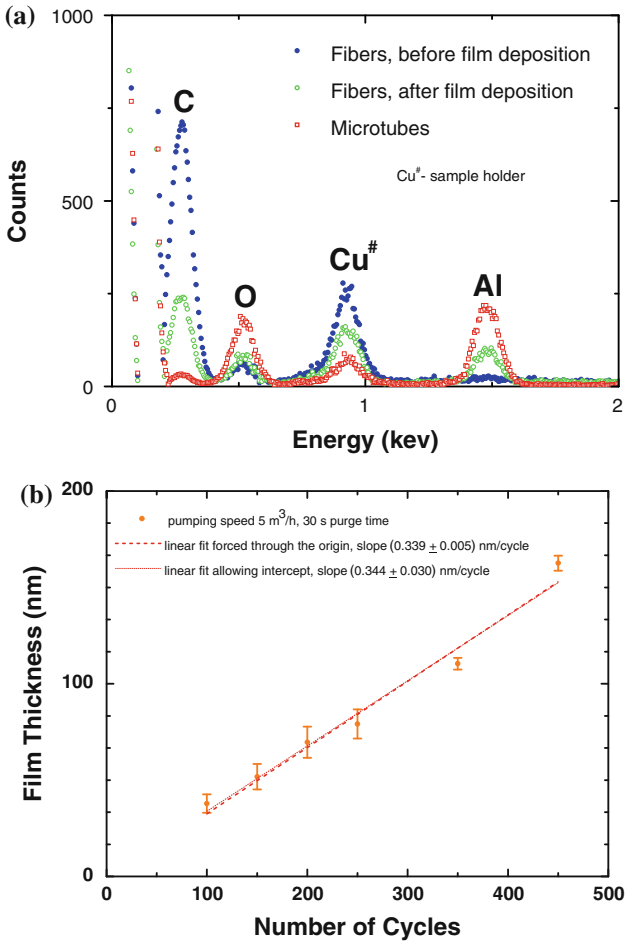

Fig. 3 (**a**) Energy dispersive X-Ray spectrum of fibers before film deposition, fibers after film deposition, and microtubes. (**b**) Film thickness as a function of deposition cycles

of amorphous and crystalline regions, the crystalline regions having to some extend preferential orientations with respect to the fiber axis [21]. Thus, the fiber exposes various functionalities to the surface enabling the physisorption and/or chemisorption of either TMA [22, 23] or water.

Films on the carbon fibers

Thin alumina films were deposited onto these carbon fibers using trimethylaluminum and water as precursors at a temperature of 77 °C in a flow type reactor via pulsed CVD. In the 1st half cycle, the fiber bundle was exposed to trimethylaluminum for 20 s followed by purging the reactor with nitrogen for 30 s. In the second half cycle it was exposed to water vapor for 20 s followed by another purging of the reactor with nitrogen for 30 s. After coating, the bundles of fibers have essentially the same morphology but are colored, see Fig. 1c, d, indicating interference of light reflected at the outer and inner interface of the films. Elemental analysis of the thin films deposited onto fibers by energy dispersive X-ray spectroscopy (EDXS) revealed a dominating carbon content as well as aluminum and oxygen (see Fig. 3a). The dominating amount of carbon was expected because of the carbon fiber, the presence of aluminum and oxygen confirms the expected alumina coating.

Various segments of fiber bundles were observed by SEM after exposing certain numbers of film deposition cycles. The fibers within the bundle are separated from each other, no bridging has been formed and the films were deposited evenly onto each individual fiber (see for example Fig. 2c). Figure 2d shows a single fiber cut after film deposition, there is a slight contrast between a part of the fiber adjacent to the front and the part further up. Obviously, close to the front, a part of the film was damaged and removed by the cutting process, exposing the carbon inside; further up the slightly more bright appearance indicates undamaged coating. Close up images of this part reveals a clear step in the surface profile. From the height of this step one can estimate the thickness of the film. The average thicknesses of the film thus estimated from various fibers are presented in Fig. 3b as a function of the number of deposition cycles. There is a linear relationship between the film thickness and the number of cycles with an average deposition rate of (0.34 ± 0.03) nm per cycle. The deposition rate is higher than the value that can be estimated theoretically for a monomolecular layer of alumina [24] which indicates that the process is a pulsed CVD rather than the strict ALD used in [18].

Microtubes

Microtubes were synthesized by removing the carbon fibers via thermal oxidation in air at temperatures exceeding 550 °C using a tube furnace. To remove the fibers, time spans between 3 and 12 h were needed, depending on coating thickness and the process temperature. 10 to 12 h were needed at 550 °C and 3 to 4 h at 900 °C. This thermal treatment was accompanied by a change in color from dark to white the overall shape and arrangement of the bundles being unaffected (see Fig. 1g, h). The change of color occurred evenly along the bundles. SEM and transmission electron microscopy (TEM) images after thermal oxidation revealed that the desired microtubes indeed were obtained (see Fig. 2e–g). The tubes are still separated from each other as were the fibers after film deposition and the inner diameters are equivalent to the diameter of the fibers. The tubes have the same inner morphology as the surface of the carbon fibers, i.e., a corrugated surface bearing grooves parallel to the fiber axis (see Fig. 2h) and irregular protuberances that were present on the fibers already before the coating process, in addition the tubes bear a few fragments

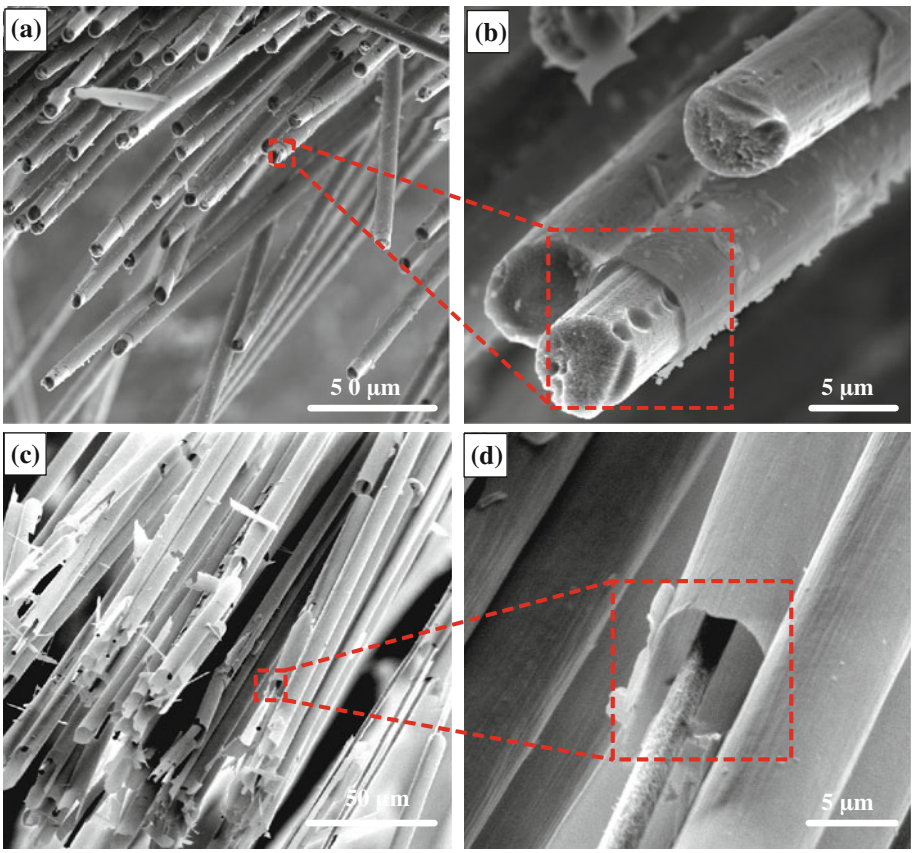

Fig. 4 Scanning electron microscopic images of bundles of coated fibers after incomplete thermal oxidation (**a**) within the TGA heating to 700 °C with a rate of 5 °C/min and subsequent annealing for 30 min, (**c**) in tube furnace at a temperature of 650 °C for 3 h, (**b**) and (**d**) close up views of (**a**) and (**c**)

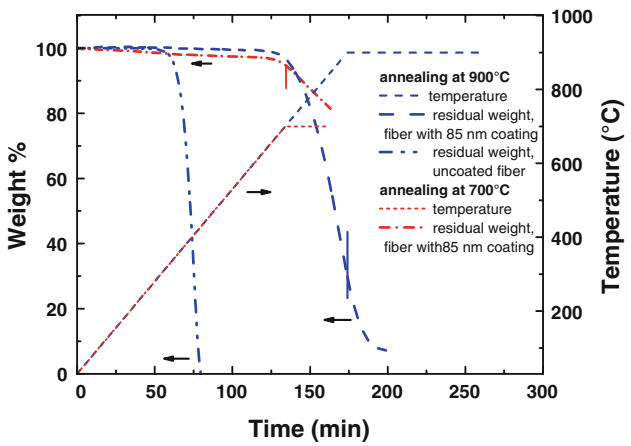

Fig. 5 Thermogravimetric analysis of uncoated and coated fibers in synthetic air. The specimens were heated to the desired temperature (700 or 900 °C, indicated by thin vertical lines) with a constant heating rate of 5 °C/min and subsequently held at that temperature

that were shattered and displaced when the tubes were cut. The maximum length of the tubes prepared was 30 cm, however, it was primarily limited by the dimension of the used furnace, and thus it will be possible to synthesize tubes longer than 30 cm.

The elemental composition of the microtubes was analyzed by EDXS which revealed aluminum and oxygen and a small amount of carbon (see Fig. 3a). The small amount of carbon was expected because of oxidative removal of the carbon fiber template, the presence of aluminum and oxygen confirms the expected alumina film. EDXS does not always yield accurate quantitative chemical compositions, especially, for lower atomic weight elements; thus the carbon, nitrogen, and hydrogen content of the microtubes were measured via elemental flash analysis. Results of this analysis indicate that the amount of carbon, hydrogen, and nitrogen within the residue of thermal oxidation were 1.61%, 0.06%, and less than 0.01%, respectively. Possibly, this small amount of hydrogen and a part of the carbon can be attributed to a decomposition product of the trimethylaluminum, and the rest of the carbon as an irremovable part of the fiber. Overall, the amount of impurities in the microtubes is low.

Compared to the previously mentioned publication [18], we obtained here centimeter long microtubes and took advantage of higher film deposition rate per cycle. In principle one can manipulate our tubes individually. If the coating would be impermeable to oxygen, oxidation of the fibers had to proceed starting from both open ends. However, in our case the coated fibers gradually turn gray at intermediate stages of oxidation, they do not turn white from the end only (see Fig. 1e, f). Furthermore, SEM images reveal that the diameter of the fibers along the whole length decreases gradually with time—see for e.g.,

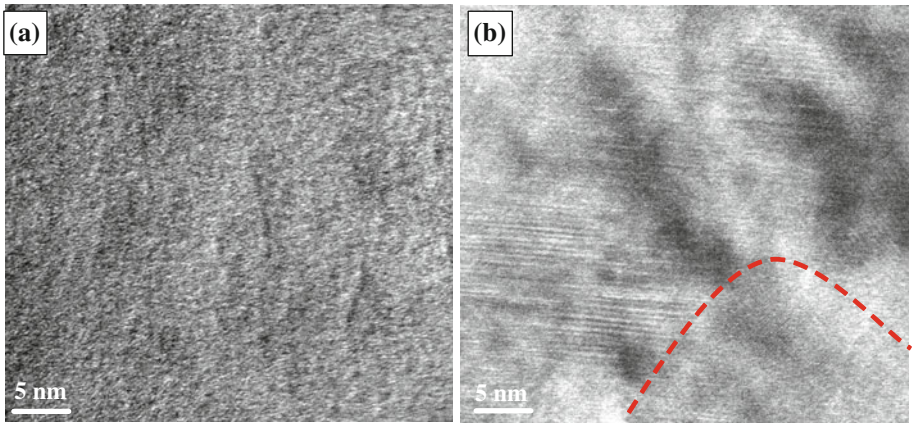

Fig. 6 High resolution transmission electron microscopic images of the walls of alumina microtubes (**a**) prepared at 550 °C and (**b**) at 900 °C

Fig. 4. Already at early stages of oxidation (20% weight loss of the coated fiber), one can observe a slight decrease of diameter of the fibers and a clear and uniform gap between the tube and the remaining fiber (see Fig. 4a, b). In addition in this early stage of oxidation one observes the formation of "pits" in the surface of the fibers. However, these pits form as well if uncoated fibers are oxidized (images not shown). Thus, they are characteristics of the fiber and not of the coating, probably indicating inhomogeneities within the fiber [21]. More extensive oxidation in a tube furnace gradually reduces the fiber diameter (see Fig. 4c, d) until they are finally completely removed. The decomposition of the coated fibers by annealing in air was repeated in a thermogravimetric analyser, heating the fibers with a constant heating rate to a desired temperature (700 and 900 °C) and annealing them further at that temperature (see Fig. 5). The uncoated fibers start to lose weight at approximately 300 °C, whereas the coated fibers start to lose weight at approximately 700 °C. This indicates that the coating slows down the decomposition by acting as a barrier between the air and the fiber and that the decomposition of the fiber is due to oxidation into gaseous carbon oxides. Thus, in our case there has to be some permeability for oxygen and combustion products at elevated temperatures. This assumption of permeability of the coating for gases is in agreement with the results presented in [18]: the layers prepared in this reference via strict ALD enable removal of the templating fibers via annealing and thus need to be permeable for gaseous products as well. Layers prepared via strict ALD usually are less permeable than those prepared via pulsed CVD. Thus, one can expect that removal of gaseous products here is more facile than the result presented in [18], however, we have seen similar oxidation behaviour in case of ALD layer, at least via thermogravimetic analysis (see Fig. 6 of ref [19]).

High resolution transmission electron microscopic (HRTEM) images reveal that tubes obtained via oxidation at 550 °C have a low degree of crystallinity (Fig. 6a) whereas the tubes obtained via oxidation at 900 °C (Fig. 6b) showed a significant degree of crystallization, even exposing details that may be interpreted as grain boundaries. This change in structure might influence the decrease of barrier properties of the layer at temperatures exceeding 700 °C.

Conclusion

In conclusion, pulsed CVD is a convenient technique which allows to coat carbon fibers at a low temperature with uniform and conformal films and gives rise to a comparatively high deposition rate (0.34 ± 0.03 nm/cycle). Thermal oxidation is an useful method to remove the carbon without affecting the alumina and thus allows to prepare tubes with morphologies similar to the fibers.

Acknowledgements We are grateful to Harry Rose, Micromanufacturing Technology, Chemnitz University of Technology, for designing the control software of the ALD reactor, Frank Diener and Frank Sternkopf from the metal-workshop, Chemnitz University of Technology, for building components of ALD reactor. We are thankful to Steffen Schulze from Solid Surfaces Analysis Group, Chemnitz University of Technology, for TEM analysis and to Thomas Mäder, Institute of Material Science and Engineering, for SEM images.

References

1. Avedisian T, Raj R (1995) US Patent 5451260, 1995
2. Hausmann D, Becker J, Wang S, Gordon RG (2002) Science 298:402
3. Uchida S, Chiba R, Tomiha M, Masaki N, Shirai M (2002) Electrochemistry 70:418
4. Ohsaki Y, Masaki N, Kitamura T, Wada Y, Okamoto T, Sekino T, Niihara K, Yanagida S (2005) Phys Chem Chem Phys 7:4157
5. Varghese OK, Gong D, Paulose M, Ong KG, Grimes CA (2003) Sens Actuators B 93:338
6. Varghese OK, Gong D, Paulose M, Ong KG, Dickey EC, Grimes CA (2003) Adv Mater 15:624

7. Fan R, Karnik R, Yue M, Li D, Majumdar A, Yang P (2005) Nano Lett 5:1633
8. Lee SB, Mitchell DT, Trofin L, Nevanen TK, Söderlund H, Martin CR (2002) Science 296:2198
9. Martin CR, Kohli P (2003) Nat Rev Drug Discov 2:29
10. Spahr ME, Bitterli P, Nesper R, Müller M, Krumeich F, Nissen HU (1998) Angew Chem Int Ed 37:1263
11. Niederberger M, Muhr H-J, Krumeich F, Bieri F, Günther D, Nesper R (2000) Chem Mater 12:1995
12. Iijima S, Ichihashi T (1993) Nature 363:603
13. Bethune DS, Kiang CH, de Varies MS, Gorman G, Savoy R, Vazquez J, Beyers R (1993) Nature 363:605
14. Schmidt OG, Eberl K (2001) Nature 410:168
15. Bae C, Yoo H, Kim S, Lee K, Kim J, Sung MM, Shin H (2008) Chem Mater 20:756
16. Caruso RA, Schattka JH, Greiner A (2001) Adv Mater 13:1577
17. Bognitzki M, Hou HQ, Ishaque M, Frese T, Hellwig M, Schwarte C, Schaper A, Wendorff JH, Greiner A (2000) Adv Mater 12:637
18. Peng Q, Sun XY, Spagnola JC, Hyde GK, Spontak RJ, Parsons GN (2007) Nano Lett 7:719
19. Roy AK, Baumann W, König I, Baumann G, Schulze S, Hietschold M, Mäder T, Nestler DJ, Wielage B, Goedel WA (2010) Anal Bioanal Chem 396:1913
20. Roy AK, Baumann W, Schulze S, Hietschold M, Mäder T, Nestler DJ, Wielage B, Goedel WA (2011) J Am Cer Soc (published online 18 Feb 2011)
21. Bai Y-J, Wang C-G, Lun N, Wang YX, Yu M-J, Zhu B (2006) Carbon 44:1773
22. Kisker DW, Stevenson DA, Miller JN, Stringfellow GB (1982) J de Phys 43:C5
23. Kisker DW, Stevenson DA (1983) J Electron Mater 12:459
24. Puurunen RL (2003) Chem Vap Depos 9:327
25. Bamford CH, Levi DL, Newitt DM (1946) J Chem Soc 468
26. Landolt H, Börnstein R, Eucken A (1960) Zahlenwerte und Funktionen aus Physik, Chemie, Astronomie, Geophysik und Technik 6th ed, vol 2. Springer, Berlin, p 61